

Figure S1: Accuracy of different algorithms as a function of resolvability of population structure. This figure is similar to Figure 1 in the main text, with results using the F-prior included. Subfigure (a) illustrates the demographic model underlying the three populations represented in the simulated datasets. Subfigure (b) compares the optimal model complexity inferred by ADMIXTURE ( $K_{cv}^*$ ), fastSTRUCTURE with simple prior ( $K_{cv}^*$ ,  $K_{\mathcal{E}}^*$ ,  $K_{\emptyset^c}^*$ ), fastSTRUCTURE with F-prior ( $K_{cv}^*$ ), and fastSTRUCTURE with logistic prior ( $K_{cv}^*$ ). Subfigure (c) compares the accuracy of admixture proportions estimated by each algorithm at the optimal value of  $K$  in each replicate.

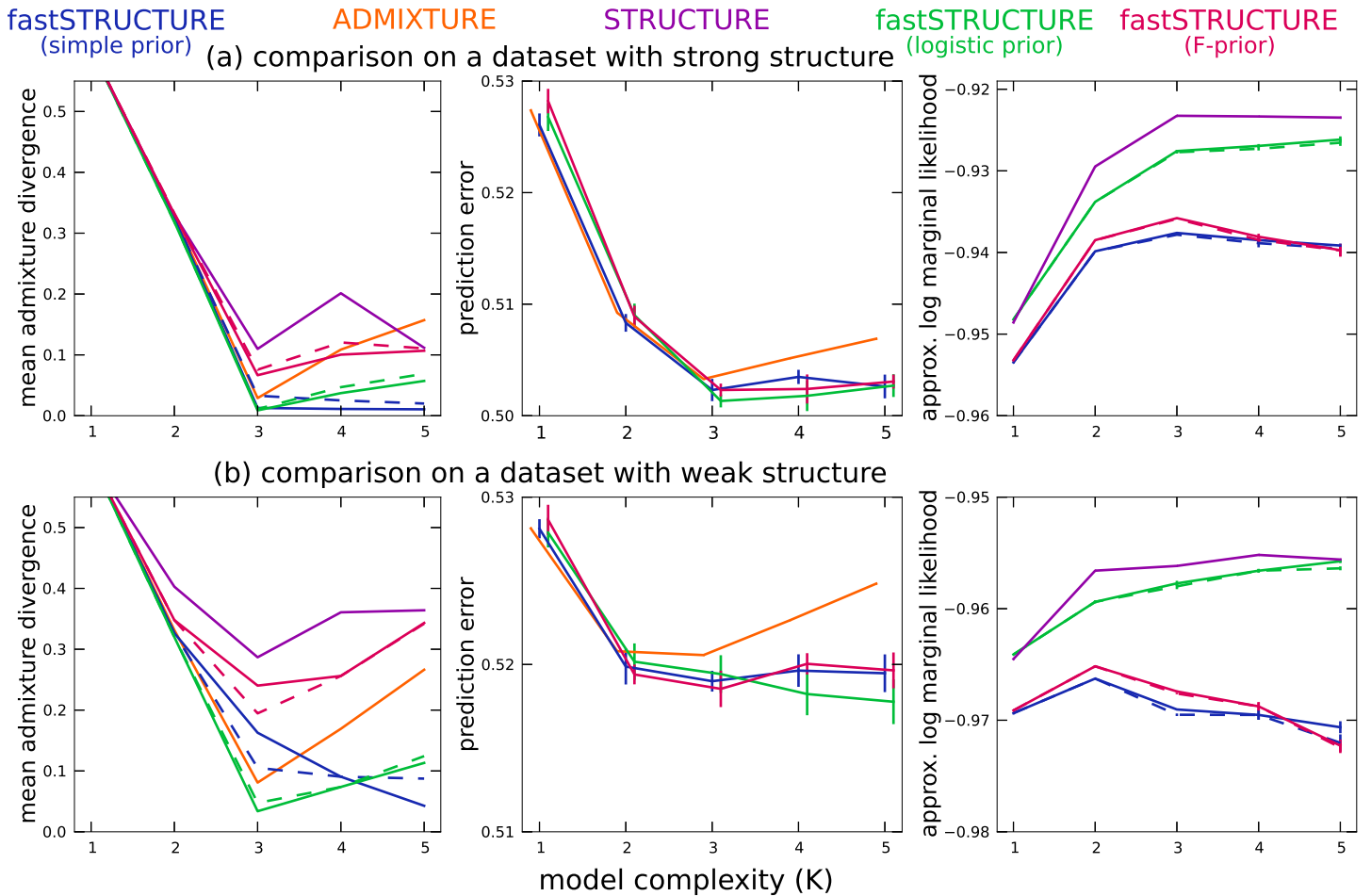


Figure S2: Accuracy of different algorithms as a function of model complexity ( $K$ ) on two simulated data sets, one in which ancestry is easy to resolve (top panel;  $r = 1$ ) and one in which ancestry is difficult to resolve (bottom panel;  $r = 0.5$ ). This figure is similar to Figure 3 in the main text, with results using the F-prior included. Solid lines correspond to parameter estimates computed with a convergence criterion of  $|\Delta\mathcal{E}| < 10^{-8}$ , while the dashed lines correspond to a weaker criterion of  $|\Delta\mathcal{E}| < 10^{-6}$ . The left panel of subfigures shows the mean admixture divergence, the middle panel shows the mean binomial deviance of held-out genotype entries, and the right panel shows the approximations to the marginal likelihood of the data computed by STRUCTURE and fastSTRUCTURE.

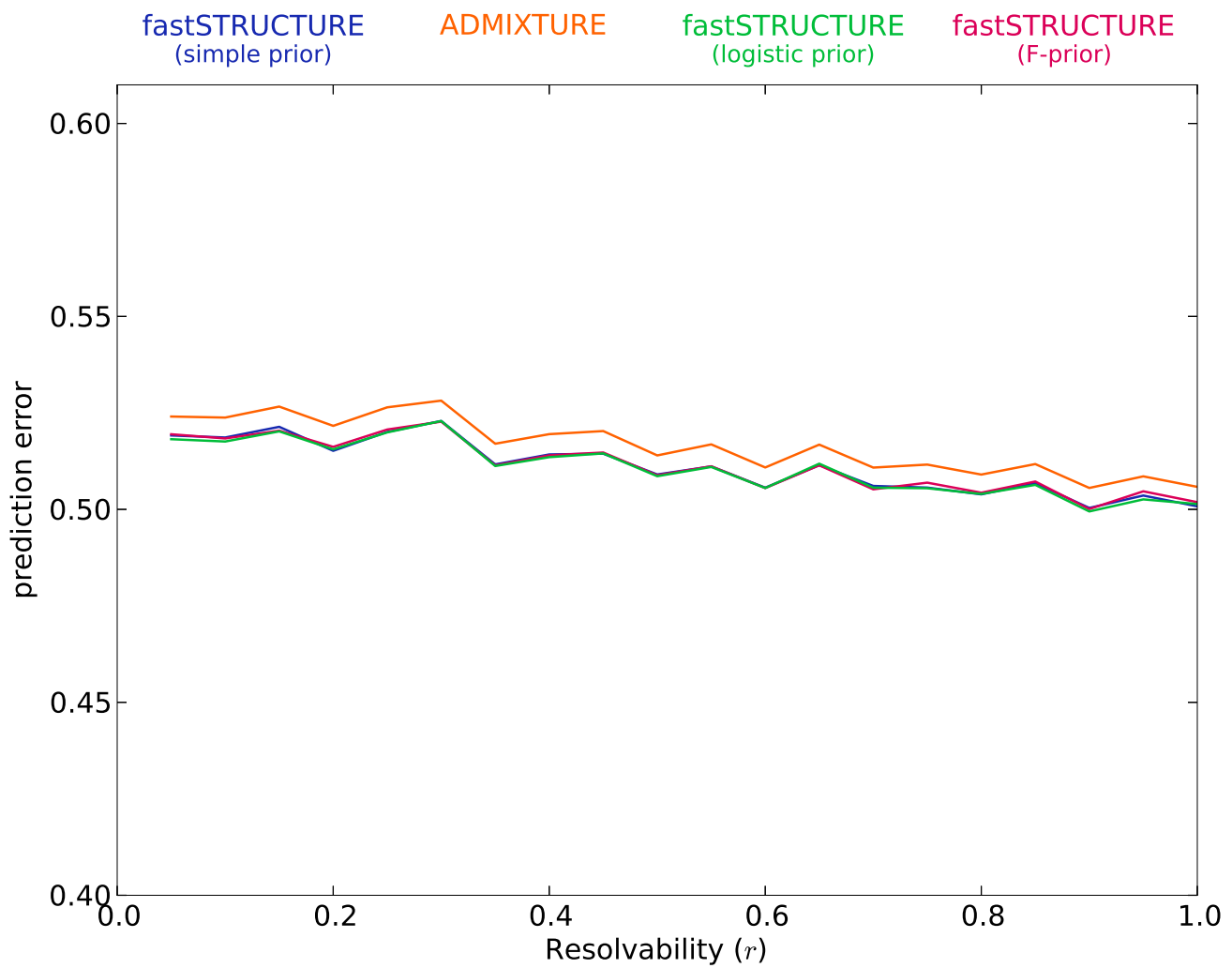


Figure S3: Prediction error of different algorithms as a function of resolvability of population structure.